JGR Atmospheres

RESEARCH ARTICLE
10.1029/2019JD030780

The Role of Clouds and Surface Heat Fluxes in the Maintenance of the 2013–2016 Northeast Pacific Marine Heatwave

Lauren Schmeisser[1], Nicholas A. Bond[1,2,3], Samantha A. Siedlecki[4], and Thomas P. Ackerman[1,2]

[1]Department of Atmospheric Sciences, University of Washington, Seattle, WA, USA, [2]Joint Institute for Study of the Atmosphere and Ocean, Seattle, WA, USA, [3]NOAA Pacific Marine Environmental Laboratory, Seattle, WA, USA, [4]Department of Marine Sciences, University of Connecticut, Groton, CT, USA

Key Points:
- During the 2013–2016 NE Pacific marine heatwave, a decrease in low cloud fraction and increase in surface radiative fluxes were observed
- Concurrently, anomalous turbulent fluxes and ocean processes offset a positive SST-cloud feedback to maintain high SST anomalies
- A balance of anomalous processes allows the atmosphere–ocean system in the NE Pacific to maintain an anomalous state for multiple years

Supporting Information:
- Supporting Information S1

Correspondence to:
L. Schmeisser,
schmeiss@uw.edu

Citation:
Schmeisser, L., Bond, N. A., Siedlecki, S. A., & Ackerman, T. P. (2019). The role of clouds and surface heat fluxes in the maintenance of the 2013–2016 Northeast Pacific marine heatwave. *Journal of Geophysical Research: Atmospheres*, *124*, 10,772–10,783. https://doi.org/10.1029/2019JD030780

Received 9 APR 2019
Accepted 14 SEP 2019
Accepted article online 10 OCT 2019
Published online 29 OCT 2019

Abstract Starting in late 2013, the Northeast (NE) Pacific Ocean experienced anomalously warm sea surface temperatures (SSTs) that persisted for over 2 years. This marine heatwave, known as "the Blob," produced many devastating ecological impacts with socioeconomic implications for coastal communities. The warm waters observed during the NE Pacific 2013/2016 marine heatwave altered the surface energy balance and disrupted ocean–atmosphere interactions in the region. In principle, ocean–atmosphere interactions following the formation of the marine heatwave could have perpetuated warm SSTs through a positive SST-cloud feedback. The actual situation was more complicated. While reanalysis data show a decrease in boundary layer cloud fraction and an increase in downward shortwave radiative flux at the surface coincident with warm SSTs, this was accompanied by an increase in longwave radiative fluxes at the surface, as well as an increase in sensible and latent heat fluxes out of the ocean mixed layer. The result is a small negative net heat flux anomaly (compared to the anomalies of the individual terms contributing to the net heat flux). This provides new information about the midlatitude ocean–atmosphere system while it was in a perturbed state. More specifically, a mixed layer heat budget reveals that anomalies in both the atmospheric and oceanic processes offset each other such that the anomalously warm SSTs persisted for multiple years. The results show how the atmosphere–ocean system in the NE Pacific is able to maintain itself in an anomalous state for an extended period of time.

1. Introduction and Background

From boreal fall of 2013 through early 2016, anomalously high sea surface temperatures (SSTs) were observed in the Northeast (NE) Pacific, appearing in the Gulf of Alaska waters and eventually affecting regions along the coastline of North America. The warm SSTs exceeded 6 °C above normal in some locations during its multiyear duration, making it the largest and longest marine heatwave (MHW) ever observed (Bond et al., 2015; Frölicher & Laufkötter, 2018; Gentemann et al., 2017; Jacox et al., 2016; Scannell et al., 2016). MHWs often have devastating ecological and economic impacts, which can increase in severity with the length and intensity of the MHW. Anomalously warm SSTs can cause coral bleaching (Hughes et al., 2017; Le Nohaïc et al., 2017), movement of marine species to cooler water (Cavole et al., 2016; Oliver, Benthuysen, et al., 2018; Wernberg et al., 2016), mass species die offs (Jones et al., 2018; Oliver, Benthuysen, et al., 2018; Garrabou et al., 2009), and harmful algal blooms (McCabe et al., 2016). For the NE Pacific MHW in particular, the harmful algal bloom associated with the event was the largest ever recorded and caused closures of many lucrative fisheries in the U.S. Pacific Northwest (Cavole et al., 2016; McCabe et al., 2016). A better understanding of MHWs, working toward the ability to forecast the intensity and duration, could improve the adaptive capacity of communities impacted by these events.

The NE Pacific 2013/2016 MHW (hereafter the NE Pacific MHW) is one of the most well-studied MHW events (Bond et al., 2015; Di Lorenzo & Manuta, 2016; Gentemann et al., 2017; Hartmann, 2015; Hobday et al., 2018; Jacox et al., 2016; Myers et al., 2018; Oliver, Perkins-Kirkpatrick, et al., 2018), making it a good case study for understanding the maintenance mechanisms of MHWs. A MHW is defined as a period when SSTs exceed an upper threshold, typically the 90th percentile relative to local climatology, for 5 days or longer (Hobday et al., 2016). This NE Pacific MHW ("the Blob") is defined as a severe MHW since SST anomalies

reached 3 times the 90th percentile differences from the local climatological SSTs (Hobday et al., 2018). MHWs are increasing in severity and frequency, and this trend will likely continue into the future due to climate change (Oliver, Donat, et al., 2018); consequently, it is prudent to understand the physical drivers that start and maintain MHWs (Frölicher & Laufkötter, 2018; Oliver, Benthuysen, et al., 2018). The onset of the high SSTs in the NE Pacific was associated with a ridge of high pressure that persisted over the Gulf of Alaska region for many weeks, stagnating winds and causing anomalous atmosphere–ocean heat fluxes (Bond et al., 2015; Gentemann et al., 2017; Hartmann, 2015). Less attention has been paid to why the anomalously warm SSTs lasted for so many years.

One possible process responsible for the maintenance of the MHW is a positive SST-cloud feedback. Many studies of the NE Pacific atmosphere–ocean system have observed concurrent increases in SSTs, decreases in low cloud fraction, and increases in incoming solar radiation at the ocean surface, suggestive of a positive SST-cloud feedback (Bellomo et al., 2014; Clement et al., 2009; Norris et al., 1998). In the subtropical Pacific off the coast of Baja California during the same MHW, Myers et al. (2018) observed a positive SST-cloud feedback and concluded that it did indeed play a role in the persistence of the anomalous SSTs. However, they also found that further north in the NE Pacific (40–50°N and 140–160°W) from January 2013 to December 2013, there was no evidence of a positive SST-cloud feedback during the onset of the MHW (Myers et al., 2018). The NE Pacific MHW offers a convenient natural experiment to study whether or not a SST-cloud feedback helped maintain the MHW in the midlatitudes—a region that was not been the focus of most previous work. Regional studies of cloud feedback are essential for understanding spatial patterns in these feedbacks- an important step in reducing our uncertainty of cloud feedbacks in climate models.

Here we expand on the work of Bond et al. (2015) and Myers et al. (2018) by studying a time period that encompasses the entire duration of the MHW (November 2013 to January 2016), using different datasets (Climate Forecast System Reanalysis [CFSR] and Global Ocean Data Assimilation System [GODAS]) and analyzing a different study region. We seek to understand the drivers contributing to the persistence of warm SST anomalies during the entire 2013–2016 NE Pacific MHW. Specifically, we address the following questions:

1. How does the atmosphere respond to anomalously warm SSTs during the NE Pacific MHW?
2. How does the atmospheric response to anomalously warm SSTs in turn affect the SST anomalies? In other words, what processes caused the warm SSTs to *persist* for multiple years?

2. Data and Methods

2.1. Reanalysis Data

Data from the National Centers for Environmental Prediction (NCEP) CFSR (Saha et al., 2010, 2014) are used to determine anomalies of SSTs, surface radiative heat fluxes, turbulent heat fluxes, and cloud fractions during the MHW. More details on the CFSR product are in the supporting information. We use reanalysis due to its complete spatial coverage, long time series, and comprehensive list of variables. CFSR was found to be the most appropriate reanalysis dataset for the NE Pacific region, based on comparisons between six reanalysis datasets and National Aeronautics and Space Administration's CERES satellite estimates of radiative flux and cloud fraction in which CFSR included the smallest errors (Schmeisser et al., 2018). An analysis using CERES-EBAF data is included in the supporting information so readers can see the sensitivity of results to dataset choice. Qualitatively, CERES and CFSR yield the same results (Table S1 and Figures S4 and S5 in the supporting information). CFSR turbulent fluxes were also compared to the OAFlux product (a dataset of best estimates of surface fluxes using satellite data and numerical weather prediction output), and the differences were small enough that the choice of dataset has minimal effect on results of this study (see the supporting information). All data are either provided as a 1°×1° gridded product or are regridded to 1°×1° resolution using linear interpolation. Monthly mean data are utilized for all analyses presented here, unless otherwise noted. Climatologies were computed by averaging data from 1979 to 2016, and anomalies were computed by subtracting the monthly mean from the monthly climatology. The MHW time period is defined from November 2013 to January 2016. Any MHW composited averages were computed by averaging data from that time period. The NE Pacific region of interest is defined here from 40 to 50°N and 130 to 150°W. We used the location of the maximum average SST anomaly to help define the study region for this analysis.

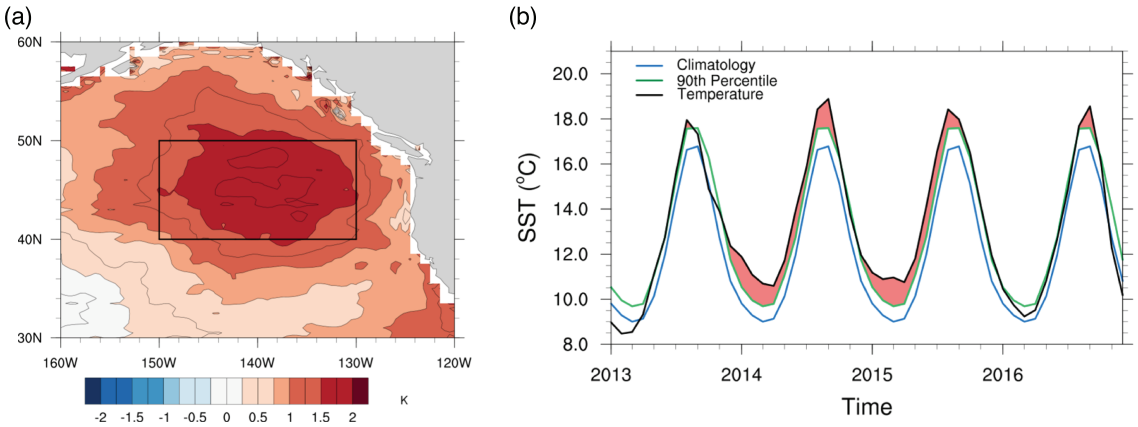

Figure 1. (a) Sea surface temperature anomaly from Climate Forecast System Reanalysis (CFSR), averaged over the time period of the marine heatwave from November 2013 to January 2016, study region outlined in black. (b) Monthly averaged sea surface temperature time series from CFSR in black, sea surface temperature (SST) monthly average climatology in blue and the monthly average 90th percentile in green. The red shading indicates any time period where SST exceeds the 90th percentile threshold and is thus defined as a marine heatwave.

2.2. MHW Identification

Here we use the MHW definition similar to Hobday et al. (2016), but we use monthly data instead of daily data. Anytime observed SSTs exceed the monthly 90th percentile threshold, it is considered a MHW. Using this method, the MHW time period for this study is defined as starting in November 2013 and ending in January 2016.

2.3. Ocean Mixed Layer Heat Budget

A mixed layer heat budget was constructed to analyze the processes contributing to anomalous SSTs during the NE Pacific MHW. Following Cronin et al. (2015), the mixed layer temperature tendency is computed from the following equation:

$$\frac{\partial}{\partial t}T = \frac{Q_o}{\rho C_p h} - u_a \cdot \nabla T - \left(w_h + \frac{dh}{dt}\right)\frac{(T - T_h)}{h} - \frac{\kappa}{h}\frac{\partial T}{\partial z}\bigg|_{z=h}$$

where T is SST, Q_o is net heat flux at the ocean surface, ρC_p is the volumetric heat capacity of water ($\rho C_p = 4.088 \times 10^6$ J° · C^{-1} · m^{-3}), h is the mixed layer depth, u_a is ocean current velocity, w_h is vertical velocity, T_h is the temperature at the bottom of the mixed layer, κ is the diffusivity constant, and z is depth. The first term on the right side of the equation represents the contribution of ocean surface net heat flux to mixed layer temperature tendency, the second term represents the contribution by horizontal advection, the third term represents entrainment at the bottom of the mixed layer, and the fourth term represents vertical diffusivity at the bottom of the mixed layer. For the purposes of this study, the third and fourth terms on the right side of the equation are combined into one term and are referred to as ocean processes at the bottom of the mixed layer. Given a lack of necessary data, this term is treated as the computational residual.

SSTs, radiative heat fluxes, and turbulent heat fluxes for computation of the mixed layer heat budget are from CFSR. Ocean current velocity and mixed layer depth data are from NCEP GODAS. The mixed layer depth is defined as the depth where the ocean temperature does not exceed more than 0.8 °C from that of the surface. This value was found to be appropriate using monthly mean data for the region of interest.

All radiative fluxes are defined with respect to the ocean mixed layer, so positive upward radiative fluxes are from the ocean to the atmosphere, and positive downward radiative fluxes are from the atmosphere to the ocean. All turbulent fluxes are defined as positive upward from the ocean to the atmosphere.

Table 1
Climatological Average[a] and Standard Deviation of Parameters From 1979 to 2016, Followed by Anomalies Composited and Averaged Over the Marine Heatwave (November 2013 to January 2016) for Sea Surface Temperature, Radiative Fluxes, Turbulent Fluxes, and Cloud Cover at Different Levels

	Climatological average and standard deviation (1979 to 2016)	Average anomaly during MHW	Average DJF anomaly during MHW	Average MAM anomaly during MHW	Average JJA anomaly during MHW	Average SON anomaly during MHW
SST (K)	285.1 ± 5.9	1.6 ± 0.2	1.3 ± 0.2	1.7 ± 0.3	1.9 ± 0.3	1.4 ± 0.3
Upward LW (W/m^2)	375.2 ± 31.3	8.2 ± 1.0	6.8 ± 0.9	8.6 ± 1.6	10.1 ± 1.6	7.6 ± 1.4
Downward LW (W/m^2)	334.0 ± 30.4	4.1 ± 1.8	4.4 ± 1.3	3.9 ± 3.7	2.8 ± 2.2	3.8 ± 2.0
Downward SW (W/m^2)	133.2 ± 74.4	7.1 ± 3.3	2.8 ± 1.7	5.9 ± 7.2	17.1 ± 7.9	5.1 ± 3.0
Net radiative flux (W/m^2)	83.1 ± 72.9	2.3 ± 1.9	0.0 ± 1.4	0.8 ± 4.2	8.8 ± 5.4	0.9 ± 2.4
Latent heat (W/m^2)	56.7 ± 40.4	7.0 ± 2.5	1.4 ± 4.5	5.9 ± 3.2	9.1 ± 3.7	17.3 ± 3.7
Sensible heat (W/m^2)	1.8 ± 16.4	1.1 ± 1.0	−3.3 ± 1.8	1.7 ± 1.1	2.0 ± 1.2	4.4 ± 1.6
Net heat flux (W/m^2)	24.5 ± 105.4	−5.8 ± 3.6	1.9 ± 6.7	−6.8 ± 6.0	−2.4 ± 5.9	−20.8 ± 5.6
Total cloud cover (%)	79.6 ± 13.5	−3.3 ± 1.3	−2.7 ± 1.1	−2.9 ± 2.3	−6.1 ± 2.9	−2.8 ± 1.4
Boundary layer cloud cover (%)	44.9 ± 18.4	−6.9 ± 1.9	−6.3 ± 1.8	−7.6 ± 4.5	−11.0 ± 2.7	−5.4 ± 2.0
High cloud cover (%)	33.4 ± 11.9	5.3 ± 1.0	5.8 ± 2.6	6.0 ± 1.3	6.0 ± 2.3	3.2 ± 1.6

Note. All values are spatially averaged over domain from 40 to 50°N and 130 to 150°W. Seasonal anomalies composited over the marine heatwave are also presented.
Abbreviations: CFSR: Climate Forecast System Reanalysis; DJF: December-January-February; JJA: June-July-August; LW: longwave; MAM: March-April-May; MHW: marine heatwave; SON: September-October-November; SW: shortwave.
[a]Climatological average is computed using monthly values from CFSR averaged over the time period from 1979–2016

3. Results

3.1. Atmospheric Response to 2013–2016 NE Pacific MHW

The CFSR data show that there was a strong anomalous atmospheric response to the warm SSTs in the NE Pacific throughout the duration of the MHW. The mean SST anomaly during the MHW averaged 1.6 K throughout the study region (Figure 1a). The duration of the NE Pacific MHW was unprecedented (Figure S2), lasting for over 2 years (Figure 1b). The atmospheric response can be seen in the MHW-composited average anomalies of surface radiative fluxes, turbulent fluxes, net heat flux, and cloud fractions during the MHW (Table 1 and Figures 2–4). Upward shortwave radiative flux anomalies are not presented here because the changes are small compared to the other radiative flux terms, and mirror changes in the downward shortwave radiative flux since ocean surface albedo remains relatively constant. More details on the processes associated with the NE Pacific MHW follow.

All CFSR surface radiative fluxes had anomalous responses to the warm SSTs in the NE Pacific. During the MHW, upward longwave radiative flux increased by 8.2 W/m^2 on average (Table 1; climatological averages and standard deviations also provided in table). This increase in upward longwave radiative flux is expected given the Stefan-Boltzmann law and, unsurprisingly, the pattern of the longwave flux anomaly mirrored the pattern of the SST anomaly (Figures 1a and 2c). During the MHW, downward longwave radiative flux increased by 4.1 W/m^2 on average. The largest downward longwave radiative flux anomalies were co-located with the largest anomalies in upward longwave radiative flux and SST (Figure 2b). The downward longwave radiative flux anomaly was due to some combination of an increase in air temperature, changes in clouds, and changes in humidity. CFSR data show changes in all of these parameters during the MHW (positive anomalies of air temperature and humidity not shown), though the relative contribution of each of these variables contributes to the increase in downward longwave radiative flux is unknown. Downward shortwave radiative flux increased by 7.1 W/m^2 during the event, likely due to the accompanying reduction in low cloud (Figure 4).

Within the region of interest, shortwave radiative flux anomalies were greatest in the southern half of the domain compared to farther north (Figure 2d). This pattern closely matches observed changes in low cloud (Figure 4). Increases in downward longwave radiative flux, upward longwave radiative flux, downward shortwave radiative flux, and upward shortwave radiative flux (not shown) result in a net radiative flux anomaly of 2.3 W/m^2 into the ocean mixed layer during the MHW (Figure 2a). Due to the spatial pattern of the shortwave radiative flux anomaly shown here, the net radiative heat flux anomaly also was

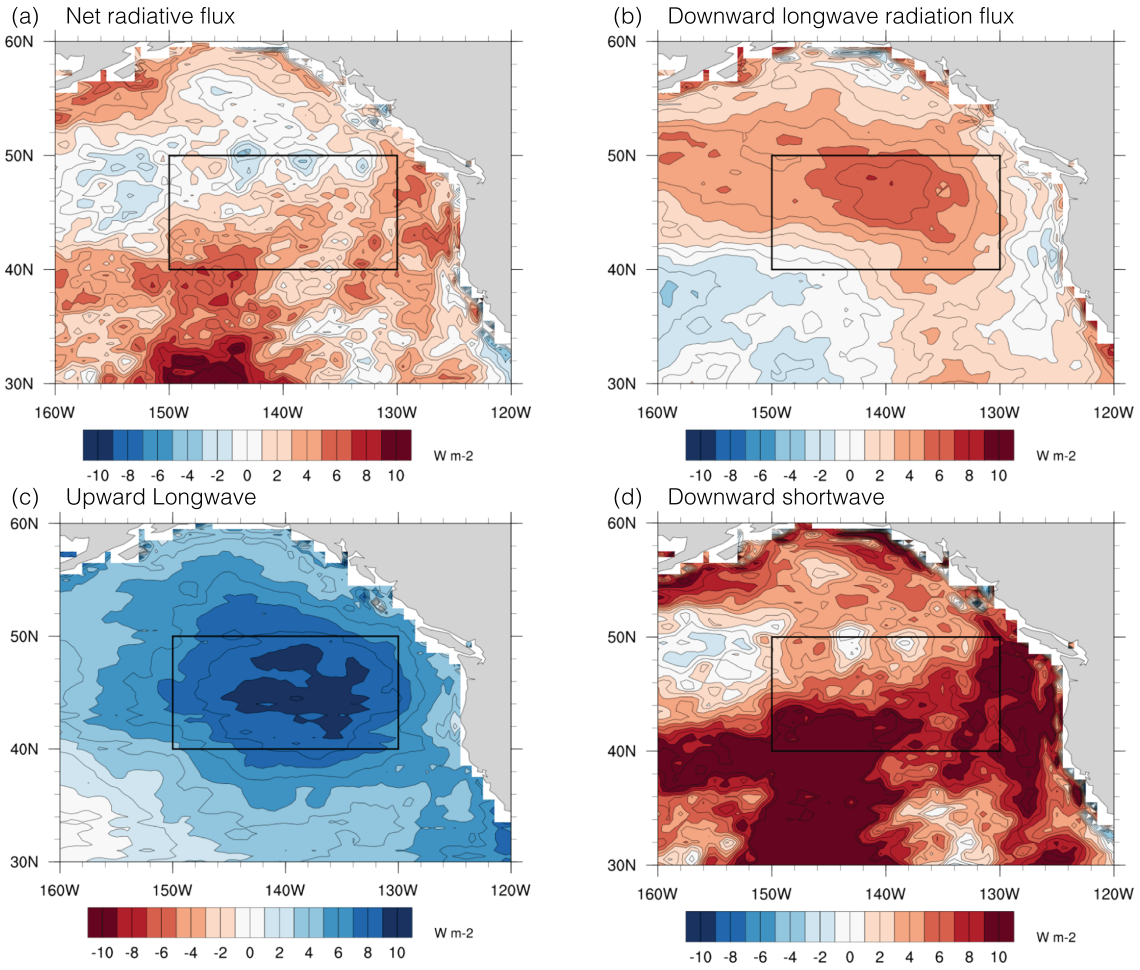

Figure 2. (a) Net radiative flux, (b) downward longwave radiative flux, (c) upward longwave radiative flux, (d) downward shortwave flux anomalies composited and averaged over marine heatwave time period (November 2013 to January 2016). The region of interest from 40 to 50°N and 130 to 150°W is boxed in black. Positive downward fluxes defined as into the ocean surface, positive upward fluxes defined as out of the ocean surface, per Climate Forecast System Reanalysis (CFSR) convention.

strongest in the southern part of the domain compared to the north (where net radiative flux anomalies were smaller or even negative).

As with radiative flux anomalies, turbulent heat flux anomalies observed during the MHW also varied spatially and seasonally. Latent heat flux anomalies were positive throughout the entirety of the domain, and averaged an additional 7.0-W/m^2 flux of energy out of the ocean mixed layer during the MHW (Figure 3a). The latent heat flux anomaly was largest during autumn (September-October-November) months throughout the MHW (an average of 17.3 Wm^{-2} energy loss from the ocean mixed layer), and smallest during winter (DJF) months throughout the MHW (an average of 1.4 Wm^{-2} energy loss from the ocean mixed layer; Table 1). Sensible heat flux anomalies were mostly positive throughout the domain and average 1.1 Wm^{-2} energy lost from the ocean mixed layer during the MHW (Figure 3b). There was also a seasonal signature in sensible heat flux anomalies with the highest positive anomaly in September-October-November (4.4 W/m^2) and a negative anomaly in December-January-February (−3.3 W/m^2; Table 1). Anomalously weak winds were observed during the MHW (Bond et al., 2015; Gentemann et al., 2017; Myers et al., 2018) and could be partially responsible for the latent and sensible heat flux anomalies during the MHW. The combination of turbulent and radiative heat fluxes yields the net flux from the ocean surface, which in this case was dominated by turbulent flux anomalies.

The average net heat flux anomaly, including both radiative and turbulent heat fluxes, was negative (−5.8 W/m^2) during the MHW and was dominated by the turbulent heat flux anomalies described above. While

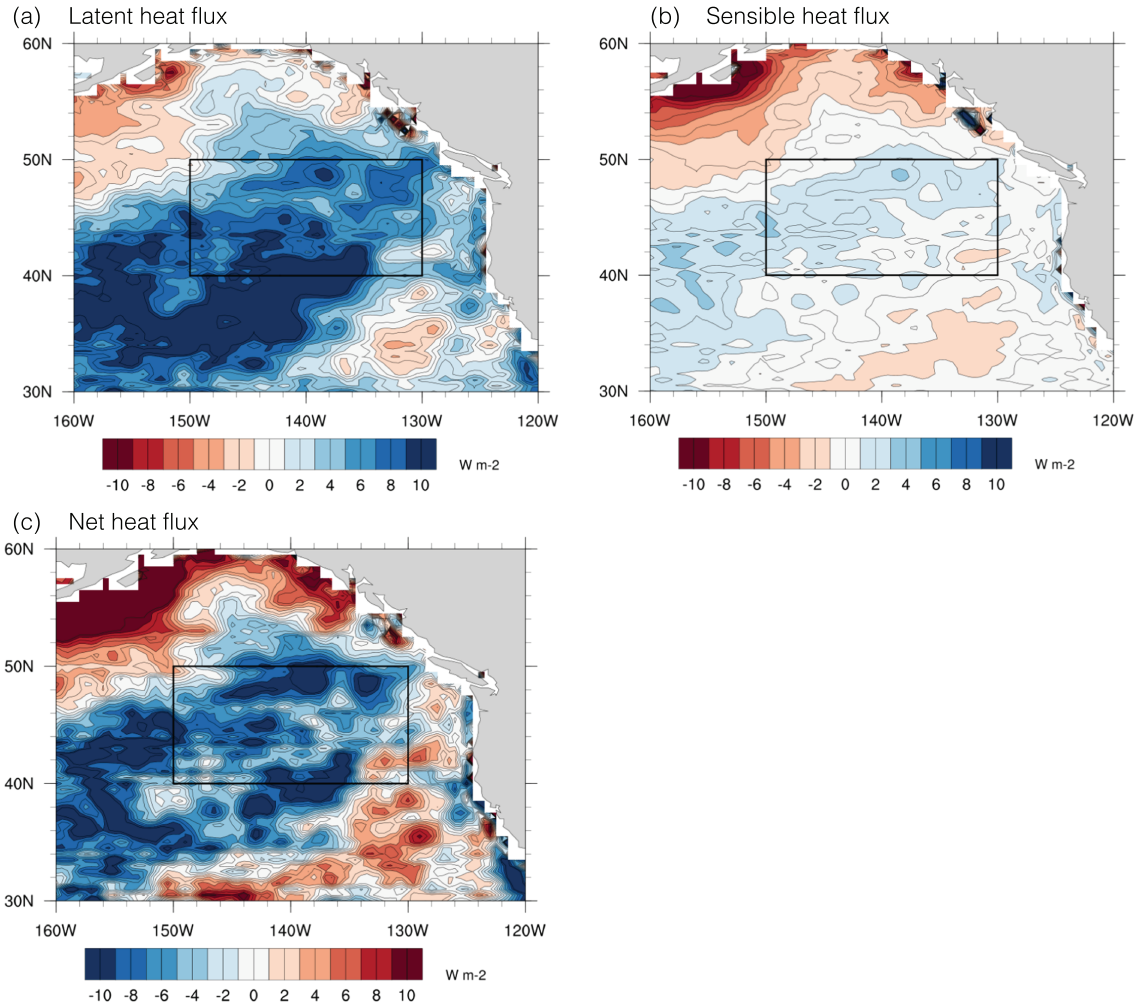

Figure 3. As in Figure 2 but for (a) latent heat flux, (b) sensible heat flux, and (c) net heat flux, including both radiative and turbulent heat fluxes. Positive turbulent fluxes defined as out of the ocean surface, positive net heat fluxes defined as out of the ocean surface, per dataset conventions.

the net radiative heat flux anomaly during the MHW provided a positive anomalous heat flux of 2.3 W/m^2 to the ocean mixed layer, the turbulent heat flux anomaly of −8.1 W/m^2 more than offset this so that the ocean mixed layer experienced net anomalous cooling (−5.8 W/m^2) due to the net anomalous heat flux alone (Figure 3c). The net heat flux anomaly was influenced by the cloud cover response to the MHW mainly through the radiative heat flux response.

Substantial cloud changes were observed which coincide with the radiative flux anomalies during the MHW. A reduction in total cloud cover occurred during the MHW, with an average anomaly of −3.3% (Figure 4a). The total cloud cover anomaly was highest during summer months (June-July-August, an anomaly of −6.4%, Table 1), when total cloud cover is highest in the NE Pacific. This summer cloud anomaly resulted in an anomalous downward radiative flux of 17.1 Wm^{-2} during a time of year when the upper mixed layer is shallow and thus the heating rate is higher. The warmer surface temperatures were in turn accompanied by enhanced heat loss (primarily due to latent heat fluxes) in the summer and fall. A reduction of boundary layer cloud cover (−6.9%) was also observed throughout the domain during the MHW (Figure 4b). The reduction in cloud cover was largest in the southern part of the domain compared to the north, and the largest anomalies were observed during the summer (June-July-August, an anomaly of −11.0%; Table 1). This reduction in low cloud was very likely the primary driver of the observed increase in shortwave radiation at the surface during the MHW. Despite reductions in low cloud cover, clouds were not reduced throughout the entirety of the atmospheric column. High cloud cover increased during the MHW by 5.3% on average

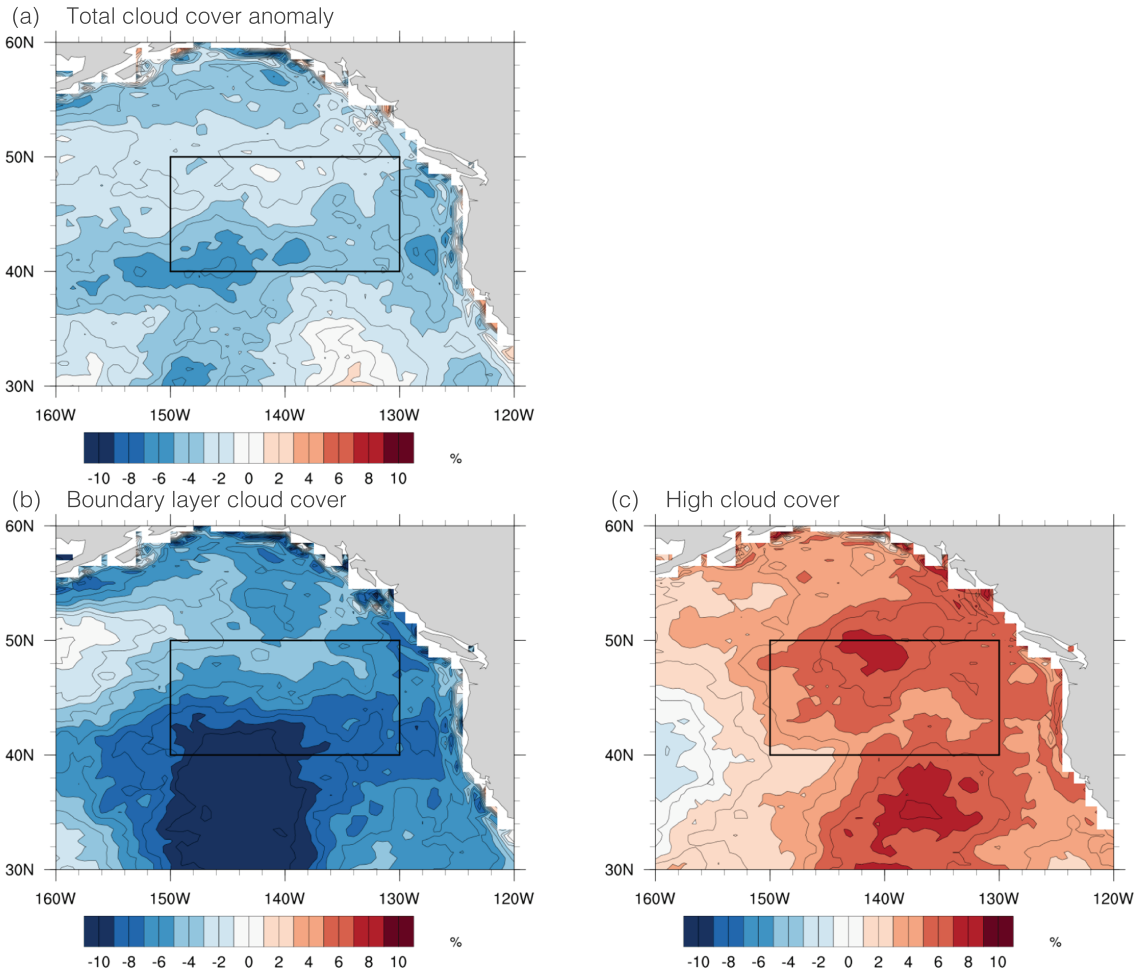

Figure 4. As in Figure 2 but for (a) total cloud cover, (b) boundary layer cloud cover, and (c) high cloud cover.

throughout the domain (Figure 4c). It is presumed that the most important effect of the high cloud changes was to contribute to an increase in the downward longwave radiative flux at the surface.

Although the elevated SSTs during the NE Pacific MHW coincided with a reduction in low cloud cover and an increase in radiative heat flux into the ocean surface, the turbulent heat flux anomalies offset the radiative heat flux anomalies such that the net heat flux anomalously cooled the ocean mixed layer (Figure 3c). Without the radiative component, however, the turbulent heat flux anomaly-driven cooling would have been more efficient.

3.2. Ocean Mixed Layer Heat Budget During 2013–2016 NE Pacific MHW

The terms of the ocean mixed layer heat budget reveal that atmospheric processes (represented in the net heat flux term) often balance the ocean processes (represented in the advection, entrainment and diffusion terms), despite varying greatly throughout the year. The time series of ocean mixed layer temperature tendency shows that it has a strong seasonality, with increasing SSTs (positive temperature tendency) from approximately February to September each year and decreasing SSTs (negative temperature tendency) from October to January (Figure 5a). This temperature tendency is largely driven by the seasonality in net heat flux, which warms SSTs in the summer when insolation is highest and cools SSTs in the winter when turbulent heat fluxes dominate (Cronin et al., 2015). Horizontal advection contributes a positive temperature tendency by advecting warmer water from the western Pacific and from lower latitudes. The bottom flux term, which is the computational residual and represents entrainment and diffusion at the bottom of the mixed layer (in addition to any errors) balances seasonality in the other terms. In summer, when the mixed layer

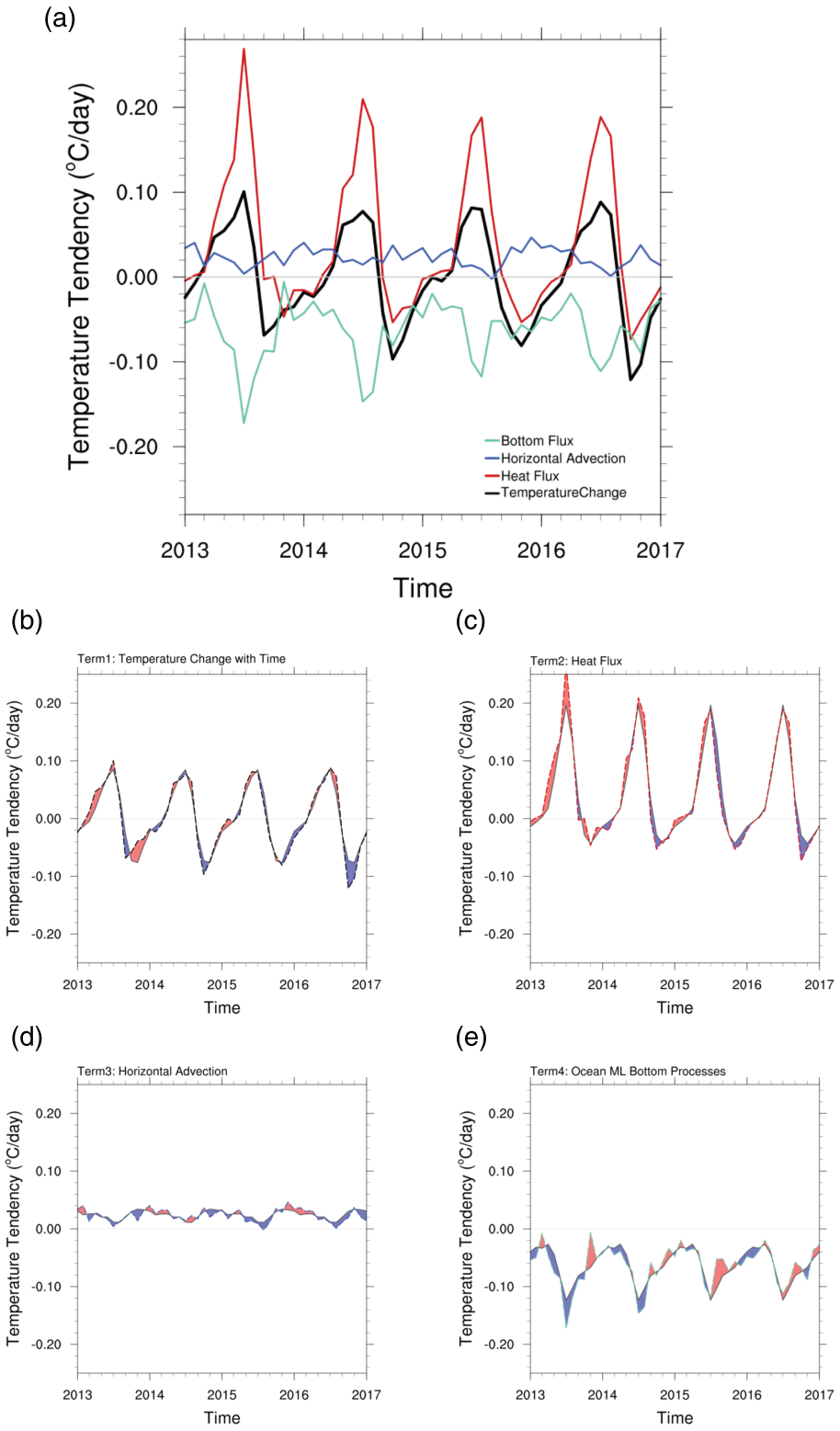

Figure 5. (a) Time series of components of ocean mixed layer heat budget–temperature change over time (black line), heat flux (red line), horizontal advection in the ocean mixed layer (blue line), and ocean processes at the bottom of the ocean mixed layer (light green line); (b) time series of temperature tendency, where the solid line is the climatology and the dashed line is observed temperature tendency 2013–2016; (c) as in (b) but for heat flux component of mixed layer heat budget; (d) as in (b) but for horizontal advection component of mixed layer heat budget; (e) as in (b) but for contribution to mixed layer heat budget by ocean processes happening at the bottom of the mixed layer. In (b)–(e), positive anomalies are shaded in red and signify that there is either additional warming (or less cooling) than typical, while negative anomalies are shaded in blue and signify that there is either less warming (or additional cooling) than typical.

Table 2
As in Table 1 But for the Four Terms of the Ocean Mixed Layer Heat Budget

		Climatological average and standard deviation (2001 to 2016)	Average monthly anomaly during MHW	Average DJF monthly anomaly during MHW	Average MAM monthly anomaly during MHW	Average JJA monthly anomaly during MHW	Average SON monthly anomaly during MHW
Temperature tendency	(°C/day)	−1.0e-4 ± 5.3e−2	-2.2e-3 ± 1.5e-2	−9.3e-4 ± 9.8e-3	2.9e-3 ± 2.8e-3	1.8e-3 ± 9.8e-3	−1.3e-2 ± 1.6e-2
	(W/m^2)	−0.30 ± 160.8	−5.7 ± 39.2	−4.9 ± 51.7	12.0 ± 11.6	1.7 ± 9.1	−24.9 ± 30.6
Net heat flux	(°C/day)	3.9e-2 ± 7.8e-2	−3.9e-3 ± 1.9e-2	1.1e-3 ± 6.0e-3	1.6e-3 ± 1.6e-3	−1.2e-3 ± 1.5e-2	−1.7e-2 ± 6.9e-3
	(W/m^2)	118.3 ± 236.6	−10.2 ± 49.7	5.8 ± 31.6	6.6 ± 6.6	−1.1 ± 14	−32.5 ± 13.2
Horizontal advection	(°C/day)	2.4e-2 ± 1.1e-2	−3.0e−3 ± 8.0e-3	-3.2e-3 ± 1.3e-2	1.0e-3 ± 3.0e-3	−6.1e−3 ± 2.1e-3	-3.9e-3 ± 1.7e-3
	(W/m^2)	72.8 ± 33.4	−7.8 ± 20.9	−16.9 ± 68.6	4.2 ± 12.5	−5.7 ± 2.0	−7.5 ± 3.3
Ocean ML bottom processes	(°C/day)	−6.3e-2 ± 3.5e-2	4.5e-3 ± 1.6e-2	3.4e-3 ± 1.5e-2	2.1e-4 ± 3.2e-3	−9.0e-3 ± 6.9e-3	8.1e-3 ± 7.7e-3
	(W/m^2)	−191.1 ± 106.2	11.8 ± 41.8	17.9 ± 79.1	0.87 ± 13.5	−8.4 ± 6.4	15.5 ± 14.7

Note. The blue shading indicates negative anomalies—less warming or more cooling than average. The orange shading indicates positive anomalies—more warming or less cooling than average.
Abbreviations: DJF: December-January-February; JJA: June-July-August; MAM: March-April-May; MHW: marine heatwave; ML: mixed layer; SON: September-October-November.

is shoaling and at its most shallow, the bottom processes are strongly cooling SSTs, while in the winter, when the mixed layer is deepest, bottom processes have a very minimal effect on SSTs in the mixed layer (Ronca & Battisti, 1997). Anomalies of the ocean mixed layer heat budget terms reveal that processes that control mixed layer SSTs were anomalous during the NE Pacific MHW (Table 2).

Furthermore, the net heat flux anomalies (section 3.1 and Figure 5c) offset positive anomalies in ocean processes (Figures 5d and 5e) in order to maintain a near-climatological SST tendency throughout the MHW. Despite the large positive anomaly in 2013 at the beginning of the heatwave, the temperature tendency remains more or less close to 1979–2016 climatology throughout the MHW, which reflects the fact that the SSTs remained elevated after the initial forcing (Figure 5b). The anomalies in each heat budget term are relatively small and not consistently either positive or negative (Figures 5b–5e). The slight seasonal variations in the anomalies of terms contributing to temperature tendency tend to offset each other, such that the temperature tendency anomaly throughout the MHW remains negligible. This analysis shows that after the initial forcing that warms SSTs and marks the onset of the MHW, these elevated upper ocean temperatures did not just relax back to climatology in a few months' time. Instead, the anomalous atmospheric and ocean processes offset and largely balanced each other (Table 2; MHW-average radiative flux anomaly of 2.3 W/m^2, latent heat flux anomaly of −8.1 W/m^2, ocean advection anomaly of −7.8 W/m^2, and mixed layer entrainment and diffusion anomaly of 11.8 W/m^2), resulting in the maintenance of the MHW for over 2 years. While the latter value was estimated as a residual, the sign of the term is reasonable. The warmth of the upper mixed layer during the MHW implies greater stratification near its base, consistent with suppressed exchanges between the mixed layer and cooler waters at depth. The demise of the MHW occurred in late 2016 during a period of enhanced cooling. The principal mechanisms were the surface heat fluxes (Figure 5c) and horizontal advection (Figure 5d) in association with anomalous winds from the northwest (not shown).

4. Discussion

Analysis of the NE Pacific 2013/2016 MHW using a combination of reanalysis data and a mixed layer heat budget shows that the atmosphere had a strong anomalous response to the warm SSTs. A positive regional, nonequilibrium SST-cloud feedback does play a role in reinforcing high SSTs but is offset by the large turbulent flux anomalies in the region. Anomalous ocean processes were largely balanced by atmospheric processes, which preserved the atypically warm SSTs, maintaining the MHW for over 2 years.

A remarkable result from this study is that the midlatitude NE Pacific atmosphere–ocean system has the ability to maintain itself in an anomalous state for multiple years through a subtle balance between oceanic and atmospheric processes. After the initial atmospheric forcing that caused the SST warming (Bond et al.,

2015), the atmosphere responded with anomalies in radiative fluxes (2.3 W/m^2) that were largely offset by anomalies in latent heat fluxes (−8.1 W/m^2) and balanced by anomalies in ocean advection (−7.8 W/m^2) and mixed layer entrainment and diffusion (11.8 W/m^2). This yielded a near-climatological SST tendency during the MHW and led to the unprecedented persistence of the warm SST anomalies. Our results also show that mechanisms that start a MHW are not necessarily the same as the combination of oceanic and atmospheric mechanisms that maintain the anomalous SSTs during a MHW or contribute to the decay of a MHW (Bond et al., 2015; Myers et al., 2018).

Myers et al. (2018) did not follow the MHW to termination and analyzed a slightly different region than the one analyzed here. Nevertheless, while magnitudes of radiative and latent heat flux anomalies during the NE Pacific MHW differed between this study and Myers et al. (2018), both analyses highlight the importance of latent heat fluxes in the mixed layer heat budget in the NE Pacific MHW. This study finds an average net radiative flux anomaly of 2.3 ± 1.9 W/m^2 additional energy into the ocean mixed layer from November 2013 to January 2016; Myers et al. (2018) find a much smaller net radiative flux anomaly 0.4 ± 1.7 W/m^2 net for the region from 40 to 50°N, 140 to 160 °W in 2013, and the 0 ± 1 W/m^2 anomaly in 2014. Here we find turbulent heat flux anomalies of 8.1 ± 3.5 W/m^2 out of the ocean from November 2013 to January 2016, while Myers et al. (2018) present turbulent heat flux anomalies of −12.7 ± 4.7 W/m^2 (into the ocean) in 2013. Results show different processes at work at the onset of the MHW (Myers et al., 2018) compared to throughout the duration of the MHW. Here we show that positive radiative flux anomalies throughout the MHW were important in maintaining the SST anomalies, contrary to conclusions in Myers et al. (2018). In addition, turbulent heat fluxes actually contributed to the onset of anomalously warm SSTs in 2013, while throughout the duration of the MHW, the turbulent fluxes provided anomalous cooling to the ocean mixed layer, which offset the positive radiative flux anomalies and yielded near-climatological SST tendencies. Still, our analyses of the NE Pacific MHW agree with Bond et al. (2015) and Myers et al. (2018) on the central role of turbulent fluxes on SSTs during the event, and that radiative anomalies associated with a SST-cloud feedback do not dominate SST tendencies in this midlatitude region.

The findings presented here have important implications for the study of SST-cloud interactions in general. While the observed reduction in low cloud concurrent with elevated SSTs during the MHW further supports ample documentation of a negative SST low cloud correlation in the NE Pacific (Clement et al., 2009; Klein et al., 1995; Klein & Hartmann, 1993; Norris, 2000; Norris et al., 1998; Norris & Leovy, 1994), the offsetting turbulent heat fluxes show that a positive SST-cloud feedback alone does not necessarily drive SST tendencies in the region. Observations of a coincident increase in SST, decrease in low cloud, and increase in incident shortwave radiative flux are not enough to infer additional SST warming. Turbulent fluxes play an essential role in determining how the change in heat flux actually affects SSTs and must be considered in analyses of SST-cloud interactions. The observed ocean–atmosphere interactions during the NE Pacific MHW closely follow the theoretical framework of Ronca and Battisti (1997), in which clouds respond to SST changes but do not further warm SSTs due to compensating turbulent heat fluxes. Ronca and Battisti (1997) find for the NE subtropical Pacific that net heat flux anomalies associated with SST anomalies are too small to in turn affect SSTs. In other words, the atmosphere responds to changes in SSTs, but the subsequent net heat flux anomalies are not large enough to feed back onto SSTs. This combined effect is more aptly described as a SST-cloud/atmosphere response than a SST-cloud/atmosphere feedback. Numerous studies claim positive SST-cloud feedback based on observations of a SST-cloud response-anomalously warm SSTs, reduction in low cloud, and increased incident solar radiation at the surface (Bellomo et al., 2014; Bellomo et al., 2016; Clement et al., 2009; Norris et al., 1998). We show here that this may not always be enough evidence to claim the presence of a true SST-cloud feedback that yields sustained anomalous SST tendencies, given the importance of turbulent fluxes and ocean processes to SST tendencies in the midlatitudes. Studies should be careful to specify the effect of SST-cloud feedback on SST tendency. In the case of the NE Pacific MHW, an observed positive SST-cloud feedback does not yield anomalous SST tendencies since turbulent fluxes counterbalance radiative fluxes to sustain SST anomalies.

In the context of other NE Pacific SST-cloud feedback studies, our work suggests that both SST-cloud feedback and turbulent flux feedback in this region likely have high spatio-temporal variability. While we show that a positive SST-cloud feedback did not dominate the mixed layer heat budget in the midlatitude NE Pacific during this MHW, there is evidence of a positive SST-cloud feedback dominating and driving the persistence of warm SSTs during the same MHW at lower latitudes in the subtropical NE Pacific (Myers et al.,

2018). Moreover, many other studies present evidence for a positive SST-cloud feedback in the NE Pacific at lower latitudes than the region studied here (Clement et al., 2009; Klein et al., 1995; Klein & Hartmann, 1993; Norris, 2000; Norris et al., 1998; Norris & Leovy, 1994). The important role of turbulent fluxes in the midlatitudes appears to be enough to dampen positive SST-cloud feedbacks that have been documented in the lower latitudes of the subtropics (Ronca & Battisti, 1997). If SST-cloud feedback indeed have such high spatio-temporal variability, more work is needed to understand what environmental variables support SST-cloud feedback. Regional studies like this are necessary to reduce the uncertainty in cloud feedback and incorporate their spatial variability more appropriately into climate models.

5. Conclusions

Reanalysis data show that the anomalously warm SSTs during the NE Pacific 2013/2016 MHW were accompanied by increases in upward longwave, downward longwave, upward shortwave, and downward shortwave radiative fluxes. The changes in downward shortwave radiative flux were associated with a reduction in low cloud fraction. The observed positive net radiative flux anomaly provides evidence for a positive SST-cloud feedback; however, this feedback does not dominate SST tendencies during the MHW. Instead, near-climatological SST tendencies were observed due to negative anomalies in turbulent fluxes that offset the radiative flux anomalies throughout the MHW. These results show the importance of turbulent fluxes to SST tendencies in the midlatitudes.

Moreover, analysis of the ocean mixed layer heat budget during the MHW reveals the essential role of ocean processes in determining the maintenance of SST anomalies during the MHW. Small anomalies in oceanic horizontal advection and processes at the bottom of the ocean mixed layer offset small anomalies in the net heat flux such that the MHW persisted for over 2 years. Through the balance in oceanic and atmospheric anomalies, the atmosphere–ocean system in the NE Pacific is able to maintain anomalous SSTs for the duration of the longest MHW ever observed.

Acknowledgments
The CFSR reanalysis data were developed by NOAA's National Centers for Environmental Prediction (NCEP). The data for this study are from the Research Data Archive (RDA), which is maintained by the Computational and Information Systems Laboratory (CISL) at the National Center for Atmospheric Research (NCAR). NCAR is sponsored by the National Science Foundation (NSF). The original data are available from the RDA (https://rda.ucar.edu/datasets/ds093.2/) in dataset number ds093.2. GODAS data are provided by the NOAA/OAR/ESRL Physical Sciences Division (PSD) in Boulder, Colorado, USA, from the website at https://www.esrl.noaa.gov/psd/. The OAFlux global ocean heat flux and evaporation products were provided by the WHOI OAFlux project (http://oaflux.whoi.edu) funded by the NOAA Climate Observations and Monitoring (COM) program. The lead author would like to thank the University of Washington IGERT Program on Ocean Change award NSF1068839 for partial funding of this work. The authors would like to thank Meghan Cronin at NOAA Pacific Marine Environmental Laboratory for her input in the early stages of this project. The authors have no real or perceived financial conflicts of interest.

References

Bellomo, K., Clement, A. C., Murphy, L. N., Polvani, L. M., & Cane, M. A. (2016). New observational evidence for a positive cloud feedback that amplifies the Atlantic Multidecadal Oscillation. *Geophysical Research Letters*, *43*, 9852–9859. https://doi.org/10.1002/2016GL069961

Bellomo, K., Clement, A. C., Norris, J. R., & Soden, B. J. (2014). Observational and model estimates of cloud amount feedback over the Indian and Pacific Oceans. *Journal of Climate*, *27*(2), 925–940. https://doi.org/10.1175/JCLI-D-13-00548.1

Bond, N. A., Cronin, M. F., Freeland, H., & Mantua, N. (2015). Causes and impacts of the 2014 warm anomaly in the NE Pacific. *Geophysical Research Letters*, *42*, 3414–3420. https://doi.org/10.1002/2015GL063306

Cavole, L. M., Demko, A. M., Diner, R. E., Giddings, A., Koester, I., Pagniello, C. M. L. S., et al. (2016). Biological impacts of the 2013-2015 warm-water anomaly in the Northeast Pacific: Winners, losers and the future. *Oceanography*, *29*(2), 273–285. https://doi.org/10.5670/oceanog.2016.32

Clement, A. C., Burgman, R., & Norris, J. R. (2009). Observational and model evidence for positive low-level cloud feedback. *Science*, *325*(5939), 460–464. https://doi.org/10.1126/science.1171255

Cronin, M. F., Pelland, N. A., Emerson, S. R., & Crawford, W. R. (2015). Estimating diffusivity from the mixed layer heat and salt balances in the North Pacific. *Journal of Geophysical Research: Oceans*, *120*, 7346–7362. https://doi.org/10.1002/2015JC011010

Di Lorenzo, E., & Manuta, N. (2016). Multi-year persistence of the 2014-2015 North Pacific marine heatwave. *Nature Climate Change*, *6*(11), 1042. https://doi.org/10.1038/nclimate3082

Frölicher, T. L., & Laufkötter, C. (2018). Emerging risks from marine heatwaves. *Nature Communications*, *9*(1), 650. https://doi.org/10.1038/s41467-018-03163-6

Garrabou, J., Coma, R., Bensoussan, N., Bally, M., Chevaldonné, P., Cigliano, M., et al. (2009). Mass mortality in Northwestern Mediterranean rocky benthic communities: effects of the 2003 heatwave. *Global Change Biology*, *15*, 1090–1103. https://doi.org/10.1111/j.1365-2486.2008.01823

Gentemann, C. L., Fewings, M. R., & García-Reyes, M. (2017). Satellite sea surface temperatures along the West Coast of the United States during the 2014-2016 Northeast Pacific marine heatwave. *Geophysical Research Letters*, *44*, 312–319. https://doi.org/10.1002/2016GL071039

Hartmann, D. (2015). Pacific sea surface temperature and the winter of 2014. *Geophysical Research Letters*, *42*, 1894–1902. https://doi.org/10.1002/2015GL063083

Hobday, A. J., Alexander, L. V., Perkins, S. E., Smale, D. A., Straub, S. C., Oliver, E. C. J., et al. (2016). A hierarchical approach to defining marine heatwaves. *Progress in Oceanography*, *141*, 227–238. https://doi.org/10.1016/j.pocean.2015.12.014

Hobday, A. J., Oliver, E. C. J., Sen Gupta, A., Benthuysen, J. A., Burrows, M. T., Donat, M. G., et al. (2018). Categorizing and naming marine heatwaves. *Oceanography*, *31*(2). https://doi.org/10.5670/oceanog.2018.205

Hughes, T. P., Kerry, J. T., Álvarez-Noriega, M., Álvarez-Romero, J. G., Anderson, K. D., Baird, A. H., et al. (2017). Global warming and recurrent mass bleaching of corals. *Nature*, *543*, 373–378. https://doi.org/10.1038/nature21707

Jacox, M. G., Hazen, E. L., Zaba, K. D., Rudnick, D. L., Edwards, C. A., Moore, A. M., & Bograd, S. J. (2016). Impacts of the 2015-2016 El Niño on the California Current System: Early assessment and comparison to past events. *Geophysical Research Letters*, *43*, 7072–7080. https://doi.org/10.1002/2016GL069716

Jones, T., Parrish, J. K., Peterson, W. T., Bjorkstedt, E. P., Bond, N. A., Ballance, L. T., et al. (2018). Massive mortality of a planktivorous seabird in response to a marine heatwave. *Geophysical Research Letters*, *45*, 3193–3202. https://doi.org/10.1002/2017GL076164

Klein, S. A., Harmann, D. L., & Norris, J. R. (1995). On the relationships among low-cloud structure, sea surface temperature, and atmospheric circulation in the summertime northeast Pacific. *Journal of Climate*, *8*(5), 1140–1155.

Klein, S. A., & Hartmann, D. L. (1993). The seasonal cycle of low stratiform clouds. *Journal of Climate*, *6*(8), 1587–1606.

Le Nohaïc, M., Ross, C. L., Cornwall, C. E., Comeau, S., Lowe, R., McCulloch, M. T., & Schoepf, V. (2017). Marine heatwave causes unprecedented regional mass bleaching of thermally resistant corals in northwestern Australia. *Nature Scientific Reports*, *7*, 14999. https://doi.org/10.1038/s41598-017-14794-y

McCabe, R. M., Hickey, B. M., Kudela, R. M., Lefebvre, K. A., Adams, N. G., Bill, B. D., et al. (2016). An unprecedented coastwide toxic algal bloom linked to anomalous ocean conditions. *Geophysical Research Letters*, *43*, 10,366–10,376. https://doi.org/10.1002/2016GL070023

Myers, T. A., Mechoso, C. R., Cesana, G. V., DeFlorio, M. J., & Waliser, D. E. (2018). Cloud feedback key to marine heatwave off Baja California. *Geophysical Research Letters*, *45*, 4345–4352. https://doi.org/10.1029/2018GL078242

Norris, J. R. (2000). Interannual and interdecadal variability in the storm track, cloudiness, and sea surface temperature over the summertime North Pacific. *Journal of Climate*, *13*(2), 422–430. https://doi.org/10.1175/1520-0442(2000)013<04222:IAIVIT>2.0.CO;2

Norris, J. R., & Leovy, C. B. (1994). Interannual variability in stratiform cloudiness and sea surface temperature. *Journal of Climate*, *7*(12), 1915–1925.

Norris, J. R., Zhang, Y., & Wallace, J. M. (1998). Role of low clouds in summertime atmosphere-ocean interactions over the North Pacific. *Journal of Climate*, *11*(10), 2482–2490. https://doi.org/10.1175/1520-0442(1998)011<2482:ROLCIS>2.0.CO;2

Oliver, E. C., Benthuysen, J. A., Bindoff, N. L., Hobday, A. J., Holbrook, N. J., Mundy, C. N., & Perkins-Kirkpatrick, S. E. (2018). The unprecedented 2015/16 Tasman Sea marine heatwave. *Nature Communications*, *8*, 16101. https://doi.org/10.1038/ncomms16101

Oliver, E. C. J., Donat, M. G., Burrows, M. T., Moore, P. J., Smale, D. A., Alexander, L. V., et al. (2018). Longer and more frequent marine heatwaves over the past century. *Nature Communications*, *9*(1), 1324. https://doi.org/10.1038/s41467-018-03732-9

Oliver, E. C. J., Perkins-Kirkpatrick, S. E., Holbrook, N. J., & Bindoff, N. L. (2018). Anthropogenic and natural influences on record 2016 marine heatwaves. *Bulletin of the American Meteorological Society*, *99*(1), S44–S48. https://doi.org/10.1175/BAMS-D-17-0093.1

Ronca, R. E., & Battisti, D. S. (1997). Anomalous sea surface temperatures and local air-sea energy exchange on intraanual timescales in the Northeastern subtropical Pacific. *Journal of Climate*, *10*, 102–117. https://doi.org/10.1175/1520-0442(1997)010<0102:ASSTAL>2.0.CO;2

Saha, S., Moorthi, S., Pan, H. L., Wu, X., Wang, J., Nadiga, S., et al. (2010). The NCEP Climate Forecast System Reanalysis. *Bulletin of the American Meteorological Society*, *91*(8), 1015–1058. https://doi.org/10.1175/2010BAMS3001.1

Saha, S., Moorthi, S., Wu, X., Wang, J., Nadiga, S., Tripp, P., et al. (2014). The NCEP climate forecast system version 2. *Journal of Climate*, *27*(6), 2185–2208. https://doi.org/10.1175/JCLI-D-12-00823.1

Scannell, J. A., Pershing, A. J., Alexander, M. A., Thomas, A. C., & Mills, K. E. (2016). Frequency of marine heatwaves in the North Atlantic and North Pacific since 1950. *Geophysical Research Letters*, *43*, 2069–2076. https://doi.org/10.1002/2015GL067308

Schmeisser, L., Hinkelman, L. M., & Ackerman, T. P. (2018). Evaluation of radiation and clouds from five reanalysis products in the Northeast Pacific Ocean. *Journal of Geophyscial Research: Atmospheres*, *123*, 7238–7253. https://doi.org/10.1029/2018JD028805

Wernberg, T., Bennnett, S., Babcock, R. C., de Bettignies, T., Cure, K., Depczynski, M., et al. (2016). Climate-driven regime shift of a temperature marine ecosystem. *Science*, *353*(6295), 169–172. https://doi.org/10.1126/science.aad8745